
First Demonstration of Leukemia Imaging with the Proliferation Marker ^{18}F -Fluorodeoxythymidine

Andreas K. Buck*¹, Martin Bommer*², Malik E. Juweid^{3,4}, Gerhard Glatting¹, Stephan Stilgenbauer², Felix M. Mottaghy¹, Melanie Schulz¹, Thomas Kull¹, Donald Bunjes², Peter Möller⁵, Hartmut Döhner², and Sven N. Reske¹

¹Department of Nuclear Medicine, University of Ulm, Ulm, Germany; ²Department of Hematology/Oncology, University of Ulm, Ulm, Germany; ³Department of Radiology, University of Iowa, Iowa City, Iowa; ⁴Holden Comprehensive Cancer Center, University of Iowa, Iowa City, Iowa; and ⁵Institute of Pathology, University of Ulm, Ulm, Germany

Acute myeloid leukemia (AML) is a neoplasm of hematopoietic stem cells with partial or complete loss of the ability to differentiate but with preserved proliferation capacity. The aim of our study was to evaluate if the *in vivo* proliferation marker 3'-deoxy-3'- ^{18}F -fluorothymidine (FLT) is suitable for visualizing leukemia manifestation sites and if ^{18}F -FLT is a surrogate marker for disease activity. **Methods:** In this pilot study, 10 patients with AML underwent pretherapeutic imaging with ^{18}F -FLT PET or ^{18}F -FLT PET/CT. The biodistribution of ^{18}F -FLT was assessed 60 min after intravenous injection of the radiotracer. Standardized uptake values were calculated for reference segments of bone marrow, spleen, and normal organs. ^{18}F -FLT PET in 10 patients with benign pulmonary nodules and the absence of malignant or inflammatory disease served as controls. **Results:** Retention of ^{18}F -FLT was observed predominantly in bone marrow and spleen and was significantly higher in AML patients than in controls (mean ^{18}F -FLT SUV in bone marrow, 11.5 and 6.6, $P < 0.05$; mean ^{18}F -FLT SUV in spleen, 6.1 and 1.8, $P < 0.05$). Outside bone marrow, focal ^{18}F -FLT uptake showed extramedullary manifestation sites of leukemia in 4 patients (meningeal disease, pericardial, abdominal, testicular, and lymph node), proven by other diagnostic procedures. **Conclusion:** This pilot study indicated that PET using ^{18}F -FLT is able to visualize extramedullary manifestation sites of AML and reflects disease activity. Because ^{18}F -FLT uptake in bone marrow is caused by a combination of both neoplastic and normal hematopoietic cells, the correlation of ^{18}F -FLT uptake in bone marrow and leukemic blast infiltration did not reach statistical significance.

Key Words: acute myeloid leukemia; nucleoside analogs; proliferation; positron emission tomography

J Nucl Med 2008; 49:1756–1762
DOI: 10.2967/jnumed.108.055335

Acute myeloid leukemia (AML) is a clonal disease of hematopoietic progenitor cells that lose the ability to differentiate and to respond to normal regulators of cellular

proliferation. Genetic factors are regarded as the most important factors for prediction of response to treatment and patient outcome (1). In the care of patients with AML—in contrast to malignant lymphoma (2)—imaging techniques based on morphologic (CT, MRI) or functional (PET, scintigraphy) alterations play only an ancillary role, for example, for management of infections or detection of uncommon manifestation sites. Extramedullary disease in lymph nodes, the central nervous system, or soft tissue seems to be of increasing significance in patients with relapse after allogeneic stem cell transplantation (3–7). To know about extramedullary manifestations is important for long-term disease control, because some of these sites may not be reached by standard chemotherapy. Standard diagnostic procedures such as lumbar puncture with cerebrospinal fluid cytology have proven to be of high specificity but lack sensitivity despite additional flow cytometry (8).

PET using the glucose analog ^{18}F -FDG enables detection of various hematologic neoplasms due to altered glucose consumption and allows assessment of response early in the course of treatment (9,10). Increased ^{18}F -FDG uptake in extramedullary leukemia has been demonstrated in case reports (11), but leukemic manifestations in areas of high glucose metabolism such as the meninges or the pericardium may not be detected by ^{18}F -FDG PET.

PET using ^{11}C - or ^{18}F -labeled DNA precursors has a potential for specific imaging of proliferation *in vivo*. ^{11}C -thymidine represents the native thymidine molecule and has been evaluated in preclinical and clinical studies (12,13). However, because of the rapid *in vivo* degradation and short half-life of ^{11}C , this tracer was regarded as inappropriate for routine clinical use. In 1998, Shields et al. introduced 3'-deoxy-3'- ^{18}F -fluorothymidine (FLT) as a thymidine analog that is resistant to *in vivo* degradation and accumulates predominantly in proliferating tissues (14). Recently, we have shown that ^{18}F -FLT is suitable for detection of malignant lymphoma and superior tumor grading (15). Because of physiologically increased uptake of ^{18}F -FLT in the bone marrow, ^{18}F -FLT PET has also been suggested for bone marrow imaging (16). More recently, our group has shown that radiolabeled thymidine analogs such as 5- ^{123}I -iodo-4'-

Received Jun. 22, 2008; revision accepted Jul. 24, 2008.

For correspondence or reprints contact: Andreas Buck, Department of Nuclear Medicine, Technische Universität München, Ismaninger Strasse 22, D-81675 Munich, Germany.

E-mail: andreas.buck@tum.de

*Contributed equally to this work.

COPYRIGHT © 2008 by the Society of Nuclear Medicine, Inc.

thio-2'-deoxyuridine (^{123}I -ITdU) can be used for induction of leukemia cell kill by mediating nanoirradiation to DNA (17).

Here, we assessed the biodistribution of ^{18}F -FLT in patients with AML and the utility of ^{18}F -FLT PET for visualizing extramedullary manifestation sites of AML and evaluating disease activity.

MATERIALS AND METHODS

Study Inclusion Criteria

This prospective study comprised 10 patients (4 men and 6 women) with a mean age of 47 y (range, 23–70 y; Table 1). Patients with high-risk AML scheduled for subsequent myeloablative treatment and bone marrow transplantation were eligible to participate in this study. One patient had newly diagnosed AML exhibiting unfavorable cytogenetics (patient 1; Table 1), 7 patients were recruited because of clinical evidence or morphologic proof of relapse, and 2 patients were recruited because of refractory disease. Ten healthy controls who were examined previously for further work-up of indeterminate pulmonary nodules served as a reference. Patients who had radio- or chemotherapy within 4 wk were excluded from this series. All patients gave written informed consent to participate in the study, which was approved by the local ethical committee. Bone marrow aspiration cytology was performed on all patients, followed by morphologic analysis, immunophenotyping, and cytogenetic studies. Two hematologists interpreted the results on the basis of the current World Health Organization classification (18).

Synthesis of ^{18}F -FLT

^{18}F -FLT was produced using the method of Machulla et al., with minor modifications (19). ^{18}F -fluoride was produced via the $^{18}\text{O}(p,n)^{18}\text{F}$ nuclear reaction by bombardment of isotopically

enriched ^{18}O - H_2O with a 16.5-MeV proton beam at a PETtrace cyclotron (GE Healthcare). The detailed synthesis protocol was described elsewhere (20).

Data Acquisition, ^{18}F -FLT PET, and ^{18}F -FLT PET/CT

In 5 patients, PET was performed using a high-resolution full-ring scanner (ECAT HR+; Siemens/CTI), which produces 63 contiguous slices per bed position. The axial field of view is 15.5 cm per bed position. Five bed positions were measured in each patient, covering a total field of view of 77.5 cm. The emission scan was started 60 min after intravenous injection of approximately 370 MBq of ^{18}F -FLT and included the base of the skull, neck, thorax, abdomen, pelvis, and proximal femora in all patients. In 3 patients, the entire skull was included in the emission scan. In patient 2, the extremities were additionally scanned. The acquisition time was 7 min per bed position. Three-minute transmission scans with a $^{68}\text{Ge}/^{68}\text{Ga}$ ring source were obtained for attenuation correction after tracer application. Images were reconstructed using an iterative reconstruction algorithm described by Schmidlin et al. (21). In the other 5 patients, integrated PET and helical CT using a PET/CT scanner (Discovery LS; GE Healthcare) was performed. The CT acquisition protocol included a low-dose CT scan (26 mAs, 120 kV, 0.5 s per rotation, 5-mm slice thickness) from the top of the skull to the mid thigh for attenuation correction, followed by the PET scan. All PET scans were acquired in 2-dimensional mode with an acquisition time of 3 min per bed position. Forty contiguous slices were acquired per bed position; the matrix size was 128×128 , and slice thickness was 3.4 mm. Images were reconstructed by an attenuation-weighted ordered-subsets expectation maximization algorithm (4 iterations and 8 subsets) followed by a postreconstruction smoothing gaussian filter (5 mm in full width at half maximum). Emission data were corrected for randoms, dead time, scatter, and attenuation, and we used the same

TABLE 1
Patient Characteristics

Patient no.	Age (y)	Sex	Leukemia subtype (World Health Organization)	Remission status	Verification of disease activity (% blasts)	Mean ^{18}F -FLT uptake	
						BM	Spleen
1	36	F	AML with abnormal bone marrow eosinophils inv(16)	Initial diagnosis	51%–75% (BM)	13.6	5.4
2	51	F	AML with multilineage dysplasia	Refractory (BM)	100% (BM)	15.6	7.5
3	48	F	AML, acute monoblastic leukemia	Relapse	40% (BM)	9.8	16.8
4	42	M	AML with t(8;21)	Relapse (BM + EM)	99% (PB)	11.0	8.6
5	43	M	AML minimally differentiated	Relapse (BM)	100% (BM)	9.5	6.4
6	23	F	AML, acute monoblastic leukemia	Relapse (BM)	50% (BM)	12.5	6.7
7	65	M	AML, acute monoblastic leukemia	Relapse (EM)	Blasts in ascites, liquor, lymph nodes, testicles	8.9*	1.9
8	54	F	AML	Relapse	80% (BM), 94% (PB)	12.4	16.8
9	70	M	AML with multilineage dysplasia	Refractory	20%–25% (BM), 5%–10% (PB)	15.4	5.8
10	36	F	AML, acute myelomonocytic leukemia	Second CR	<5% (BM)	8.2	2.3
11	38	M	AML, minimally differentiated	First CR, graft rejection	<5% (BM)	0.7	0.6

*Extramedullary lesion.

BM = bone marrow; EM = extramedullary lesion; PB = peripheral blood; CR = complete remission.

reconstruction algorithm as was applied for the conventional PET data. Patients serving as controls were imaged with ^{18}F -FLT PET using the same protocol as was mentioned above without CT coregistration.

Image Interpretation and Quantification of ^{18}F -FLT Uptake

All images were evaluated by 2 experienced nuclear medicine physicians. Focal ^{18}F -FLT uptake in organs with usually mild homogeneous activity or in lymph nodes that usually present without tracer uptake were interpreted as potential manifestation sites of leukemia. Circular regions of interest were drawn containing the area with focally increased ^{18}F -FLT uptake to calculate respective standardized uptake values (^{18}F -FLT SUV). A single circular region was used for SUV calculation of disease manifestation sites. Mean and maximum SUVs were calculated for bone marrow (lumbar vertebra 4) and spleen, and mean values were calculated for reference segments of the lungs, liver, kidneys, intestines, bone (skull), and brain using the same approach as for leukemia manifestation sites.

Data Analysis

After completion of the study, the results of clinical tests indicating disease activity, morphometry, cytochemistry, cytogenetics, and ^{18}F -FLT PET findings were correlated. GraphPad Prism software (version 4.03; GraphPad) was used for statistical analyses. Data are presented as mean, median, range, and SD. ^{18}F -FLT uptake in bone marrow and spleen in leukemia patients and healthy controls was compared using the Wilcoxon signed rank test. Differences were considered statistically significant at a *P* level of less than 0.05. Linear regression analysis was performed to test for a potential correlation between the number of blasts identified at bone marrow puncture (BMP) and ^{18}F -FLT uptake in bone marrow.

RESULTS

Patients

In 9 of 10 patients, reference methods indicated active disease. One patient with a history of acute myelomonocytic leukemia (patient 10) was included because of clinical suspicion of relapse; however, bone marrow biopsy revealed a second complete remission. The majority of patients were recruited because of relapse of AML (Table 1). Two patients had refractory disease with leukemic blast infiltration of 80% (patient 2) or 100% (patient 9). One patient was recruited with an initial diagnosis of AML and unfavorable cytogenetics (patient 1). Outside the study protocol, 1 patient underwent ^{18}F -FLT PET 4 wk after subsequent myeloablative radiochemotherapy, bone marrow transplantation, and transplant failure (patient 11).

Imaging AML with ^{18}F -FLT PET

In all patients with AML, bone marrow represented the organ with the highest uptake of the thymidine analog ^{18}F -FLT (Figs. 1–3). Four patients presented with ^{18}F -FLT uptake in the proximal femora and humeri not visible in controls, indicating bone marrow expansion (Fig. 2). Extensive bone marrow expansion was present in patient 2. A whole-body PET scan showed intense tracer uptake also in the bone marrow cavity of the distal femora, tibiae, and fibulae (Fig. 1). Of note, no tracer uptake in the skull or in the forearm skeleton was observed, indicating specific retention of ^{18}F -FLT in bone marrow. Additionally, focal uptake in projection of the right testicle was observed. A testicular manifestation of leukemia was further confirmed cytologically in this patient (Fig. 1).

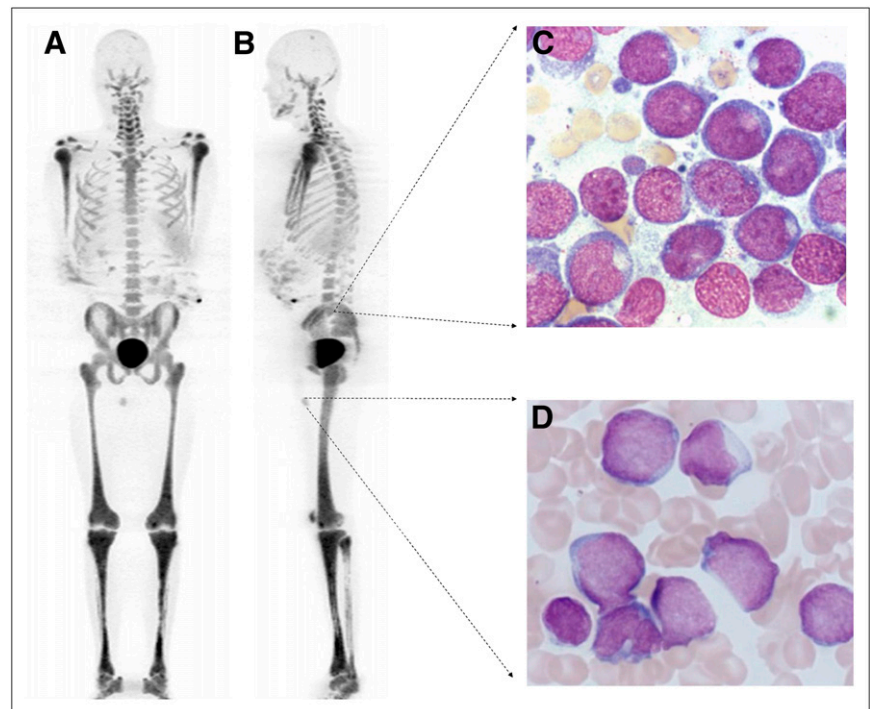


FIGURE 1. (A and B) Biodistribution of in vivo proliferation marker ^{18}F -FLT in patient with refractory AML (patient 4) 60 min after injection of radiotracer (whole-body view [3-dimensional], maximum-intensity projection). Shown are intense uptake of ^{18}F -FLT in hematopoietic bone marrow of central bones and extensive bone marrow expansion with intense tracer uptake. Tracer uptake is absent from bones not containing hematopoietic marrow (forearms and skull). Scans also indicate intense focal extramedullary ^{18}F -FLT uptake in projection of right testicle. (C) Hematoxylin staining of peripheral blood demonstrating 99% leukemic blasts. (D) Biopsy verification of testicular leukemia manifestation.

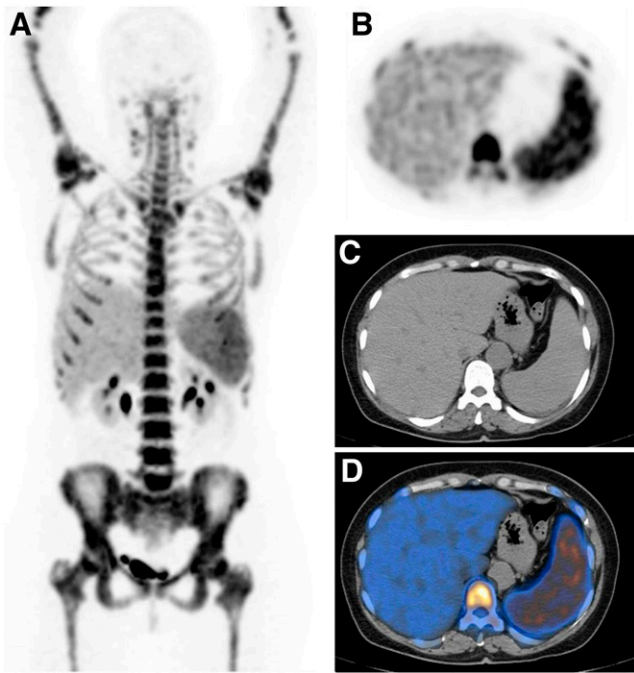


FIGURE 2. One of 2 typical distribution patterns of ^{18}F -FLT in patient with initial diagnosis of AML. (A) ^{18}F -FLT PET (whole-body view [3-dimensional], maximum-intensity projection) demonstrating intense tracer uptake in bone marrow and spleen. Distribution pattern in other organs is normal, as observed in controls. (B) Transaxial section of ^{18}F -FLT PET demonstrating intense tracer uptake in bone marrow and spleen. (C) Corresponding section of helical CT demonstrating enlarged spleen. (D) Fused image (^{18}F -FLT PET/CT).

The spleen was the organ with the second highest uptake of ^{18}F -FLT (Fig. 2; Table 1). In 6 patients with high ^{18}F -FLT uptake in the bone marrow and spleen, no extramedullary focal lesions were identified at ^{18}F -FLT PET. A different biodistribution pattern was observed in 4 patients also presenting with extramedullary lesions having focally increased ^{18}F -FLT uptake. Increased meningeal tracer uptake indicated meningeal disease in 2 patients, as was further confirmed cytologically (Fig. 3). Lymph node manifestations were visualized in 2 patients; manifestations in the thyroid, pericardium, and abdomen in another patient (Fig. 3). Interestingly, after concomitant myeloablative treatment and transplant failure, no uptake of ^{18}F -FLT was present in the bone marrow and spleen in 1 patient (Fig. 4).

Group Comparison of ^{18}F -FLT Biodistribution

Semiquantitative evaluation of ^{18}F -FLT uptake in bone marrow returned an average mean SUV of 11.5 ± 3.1 , which was significantly higher than in controls (mean ^{18}F -FLT SUV, 6.6 ± 1.2 , $P < 0.05$; Fig. 5). The average maximum ^{18}F -FLT value was also significantly higher (13.9 ± 4.5 vs. 9.7 ± 2.1 , $P < 0.05$). Both mean and maximum ^{18}F -FLT SUVs were significantly higher in the spleen, which showed only background activity in controls (mean ^{18}F -FLT SUV, 6.1 ± 4.5 and 1.8 ± 0.7 , $P < 0.05$; maximum ^{18}F -FLT SUV, 7.6 ± 5.9

and 3.1 ± 2.3 , $P < 0.05$; Fig. 5). However, there was an overlap of bone marrow or spleen ^{18}F -FLT uptake in patients with leukemia and in controls (Fig. 6).

Interestingly, retention of ^{18}F -FLT in the liver was significantly lower in AML patients than in controls (average mean ^{18}F -FLT SUV, 3.4 ± 1.1 and 5.0 ± 1.9 ; average maximum ^{18}F -FLT SUV, 4.2 ± 1.5 and 6.5 ± 2.5 ; $P < 0.05$). Biodistribution of ^{18}F -FLT in other normal organs was similar to that of controls. Accordingly, statistical analysis did not reveal significant differences of ^{18}F -FLT biodistribution in the lungs, intestines, kidneys, brain, or bone (Fig. 5).

Correlation of ^{18}F -FLT Uptake in Bone Marrow and Number of Blasts Identified at BMP

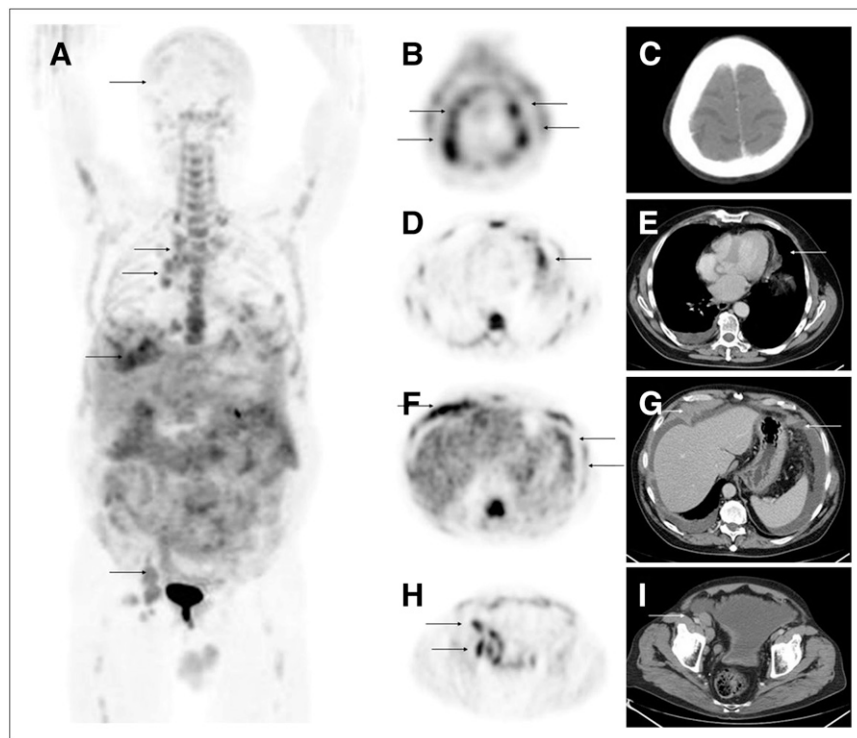
Linear regression analysis of bone marrow uptake of ^{18}F -FLT and number of leukemic blasts identified by BMP revealed no significant correlation for either mean ^{18}F -FLT SUV ($r^2 = 0.24$, $P = 0.22$) or maximum ^{18}F -FLT SUV ($r^2 = 0.23$, $P = 0.18$).

DISCUSSION

Recently, the thymidine analog ^{18}F -FLT was suggested for noninvasive assessment of proliferation and more specific imaging of a variety of solid neoplasms, including lymphoma (15,20,22–24). To our knowledge, this was the first study showing the biodistribution of ^{18}F -FLT in patients with AML. Here, we have demonstrated that ^{18}F -FLT PET is feasible for noninvasive visualization of leukemia manifestation sites. An interesting finding is a varying distribution pattern in patients with AML. Whereas the majority of patients showed intense uptake of the radionucleoside in bone marrow and spleen, extramedullary lesions were detected in 4 patients. Because lymph node basins, spleen, abdomen, mediastinum, thyroid, long bones, and brain present with missing or only marginal background activity in controls, lesions with focally increased ^{18}F -FLT uptake reflecting elevated proliferative activity could easily be detected by visual image interpretation. It remains to be determined if knowledge of extramedullary manifestation sites affects the therapeutic strategy or estimation of individual prognosis. However, these initial results warrant an analysis of a larger series of patients.

Besides visualization of leukemia manifestation sites, ^{18}F -FLT potentially represents an imaging biomarker for disease activity. The significantly higher uptake of ^{18}F -FLT in bone marrow and spleen observed in patients with relapsed, refractory, or untreated leukemia than in controls is presumably related to deregulated cell cycle progression of leukemic blasts. Recently, our group demonstrated rapid uptake of ^{18}F -FLT in an aggressive lymphoma cell line (DoHH2) (23) and of the related nucleoside ^{123}I -ITdU in HL60 leukemia cells (17). Leukemic blasts exhibit a more than 10-fold overexpression of thymidine kinase 1, which is a key enzyme for intracellular trapping of nucleosides such as ^{18}F -FLT (25,26). Also, nucleoside transporters (ENT-1) are markedly overex-

FIGURE 3. A second distribution pattern of ^{18}F -FLT in AML patients with active disease. Maximum-intensity projection of ^{18}F -FLT PET shows moderate ^{18}F -FLT uptake in bone marrow (A). Also visible are intense meningeal ^{18}F -FLT uptake (B), pericardial/mediastinal uptake (D), peritoneal uptake (F), and iliac uptake (H). Corresponding CT sections indicate no intracranial pathology (C) but pericardial effusion and mediastinal lymphadenopathy (E), peritoneal effusion (G), and enlarged iliac lymph nodes (I). Meningeal disease and further extramedullary leukemia manifestation sites (peritoneal and iliac lymph nodes) have been verified morphologically.



pressed, facilitating uptake of nucleosides such as cytosine arabinoside or ^{18}F -FLT (27).

In a pilot study, we recently demonstrated proliferation-dependent ^{18}F -FLT uptake in a follicular lymphoma cell line (23) and in a mouse lymphoma xenotransplant model (28). In a first clinical trial comprising 34 patients with low- or high-grade lymphoma, linear regression analysis indicated a

significant correlation between ^{18}F -FLT uptake and proliferation fraction as indicated by Ki-67 immunostaining ($r = 0.84$, $P < 0.0001$) (15). A similar correlation between ^{18}F -FLT retention and proliferation fraction was described in other solid tumors (20,24). However, because normal bone marrow also shows a physiologically increased proliferation rate and therefore increased ^{18}F -FLT uptake (20), the proliferative activity of leukemic blasts and normal bone marrow cannot be distinguished with ^{18}F -FLT PET. This is particularly the case in the posttreatment situation, which applies to 9 of 10 patients of our series. Accordingly, there was only a tendency toward higher retention of ^{18}F -FLT in bone marrow containing high numbers of leukemic blasts—a difference that did not reach statistical significance ($r^2 = 0.24$, $P = 0.22$). The lack of a strong correlation between the ^{18}F -FLT SUV and blasts in the bone marrow suggests that ^{18}F -FLT uptake is not related exclusively to the neoplastic compartment. A more valid assessment of the ability of ^{18}F -FLT to assess disease activity and extent should be evaluated in patients with newly diagnosed AML.

Imaging proliferation in leukemia potentially enables estimation of response to treatment and patient outcome, which has been shown recently in clinical trials including patients with malignant lymphoma, breast cancer, or glioma (29–33). In an animal model of fibrosarcoma, it was reported that ^{18}F -FLT uptake decreased early after antiproliferative treatment with 5-fluorouracil or cisplatin (30). In a mouse lymphoma xenotransplant model, a significant decrease in ^{18}F -FLT uptake had already been observed 48 h after chemotherapy with cyclophosphamide (28). However, data are

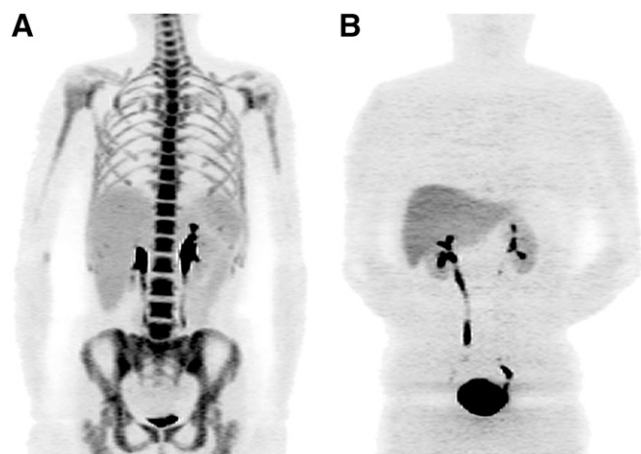


FIGURE 4. (A) Maximum-intensity projection (MIP) of ^{18}F -FLT PET in patient 9 with active disease and intense tracer uptake in bone marrow and spleen. (B) MIP of ^{18}F -FLT PET in patient 11 (not included in prospective study collective) after myeloablative treatment. At time of imaging, failure of bone marrow transplantation was diagnosed. No tracer uptake in bone marrow could be observed; administered activity was completely excreted by liver and kidneys.

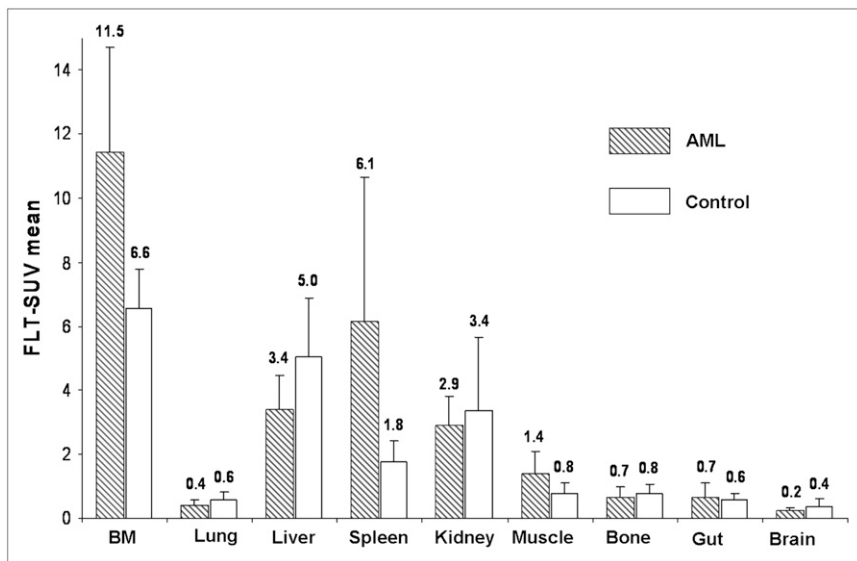


FIGURE 5. Biodistribution of ^{18}F -FLT in bone marrow, spleen, and normal organs in patients with leukemia (10 patients) and in controls (10 patients). Mean uptake values of ^{18}F -FLT are shown. Significantly higher ^{18}F -FLT uptake in bone marrow ($P < 0.05$) and spleen, and significantly lower ^{18}F -FLT uptake in liver, was seen in leukemia patients than in controls ($P < 0.05$).

preliminary, and clinical trials comprising more patients are needed to further validate ^{18}F -FLT as a marker for therapy response.

In a patient with temporary transplant failure after myeloablative chemoradiotherapy, no ^{18}F -FLT accumulation in bone marrow or spleen was observed, further illustrating the selective uptake of ^{18}F -FLT in proliferating tissues (Fig. 4). The selectivity of ^{18}F -FLT also suggests a therapeutic role of radiolabeled nucleosides. Antimetabolites such as cytosine arabinoside are standard drugs for induction treatment of leukemia but are not potent enough to maintain long-term disease-free survival (34). Coupling Auger-electron-emitting isotopes may be appropriate for nanoirradiation of DNA and entire leukemic cell kill. Recently, our group demonstrated specific induction of apoptosis and leukemic cell kill with the Auger-electron-emitting radionucleoside ^{123}I -ITdU (17). These in vitro results are encouraging and will be recapitulated in animal models and potentially in the human disease.

Several limitations have to be considered when transferring our results to the clinic. Our results apply to a pilot study comprising 10 patients only. The patient collective was also

heterogeneous and did not cover all genetic subtypes of AML. As previously reported for the standard radiotracer ^{18}F -FDG, false-positive findings may also occur using ^{18}F -FLT as a PET tracer because an increased proliferation rate is not specific to malignant tumors. ^{18}F -FLT acts as a chain terminator and is only marginally incorporated into DNA and therefore not a direct measure of proliferation (22). In vitro studies indicate that ^{18}F -FLT uptake is closely related to thymidine kinase 1 activity and respective protein levels (35), as well as to expression of nucleoside transporters in the cellular membrane (36). ^{18}F -FLT is considered to reflect thymidine kinase 1 activity and, hence, S-phase fraction rather than DNA synthesis. Both thymidine kinase and ENT are overexpressed in leukemia, facilitating preferential uptake of ^{18}F -FLT. However, the detailed uptake mechanism of ^{18}F -FLT is yet unknown, and the influence of membrane transporters and various nucleoside metabolizing enzymes remains to be determined. ^{18}F -FLT undergoes glucuronidation leading to enhanced liver uptake (15), which was also observed in our series. Because of negligible background uptake of ^{18}F -FLT in the brain and the skull (Figs. 1–3 and 5),

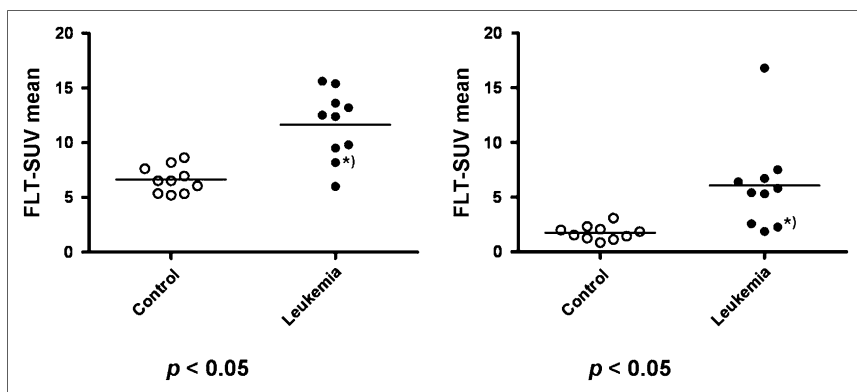


FIGURE 6. (A) Scattergram of mean ^{18}F -FLT SUVs indicating significantly higher ^{18}F -FLT uptake in bone marrow of patients with leukemia (10 patients) than in controls (10 patients, $P < 0.05$), with some overlap between groups. (B) Significantly higher ^{18}F -FLT uptake in spleen of patients with AML than in controls ($P < 0.05$). *) indicates values of patient 10 with second complete remission.

specific imaging of proliferation may be appropriate for detection of meningeal disease, which could be demonstrated in 2 members of the patient collective. However, the numbers were small, and the sensitive detection of meningeal disease may not hold up in a larger series.

CONCLUSION

We have demonstrated preferential uptake of ^{18}F -FLT in leukemia manifestation sites indicating that molecular imaging of leukemia based on deregulated cell cycle progression is feasible. Implications for clinical management and assessment of individual prognosis need to be addressed in a larger series.

ACKNOWLEDGMENT

This work was supported in part by grant Bu-1424/1 (KFO 120, P3) from Deutsche Forschungsgemeinschaft (DFG, German Research Foundation).

REFERENCES

- Estey E, Dohner H. Acute myeloid leukaemia. *Lancet*. 2006;368:1894–1907.
- Kwee TC, Kwee RM, Nievelstein RA. Imaging in staging of malignant lymphoma: a systematic review. *Blood*. 2008;111:504–516.
- Yildirim I, Uckan D, Cetin M, Tuncer M, Tezcan I. Isolated testicular and bone relapse in children with acute myeloblastic leukemia and chronic graft versus host disease after allogeneic BMT. *Turk J Pediatr*. 2007;49:206–209.
- Owonikoko T, Agha M, Balassanian R, Smith R, Raptis A. Gemtuzumab therapy for isolated extramedullary AML relapse following allogeneic stem-cell transplant. *Nat Clin Pract Oncol*. 2007;4:491–495.
- Kobayashi R, Tawa A, Hanada R, Horibe K, Tsuchida M, Tsukimoto I. Extramedullary infiltration at diagnosis and prognosis in children with acute myelogenous leukemia. *Pediatr Blood Cancer*. 2007;48:393–398.
- Kikushige Y, Takase K, Sata K, et al. Repeated relapses of acute myelogenous leukemia in the isolated extramedullary sites following allogeneic bone marrow transplantations. *Intern Med*. 2007;46:1011–1014.
- Potenza L, Luppi M, Riva G, et al. Isolated extramedullary relapse after autologous bone marrow transplantation for acute myeloid leukemia: case report and review of the literature. *Am J Hematol*. 2006;81:45–50.
- Bromberg JE, Breems DA, Kraan J, et al. CSF flow cytometry greatly improves diagnostic accuracy in CNS hematologic malignancies. *Neurology*. 2007;68:1674–1679.
- Juweid ME, Cheson BD. Positron-emission tomography and assessment of cancer therapy. *N Engl J Med*. 2006;354:496–507.
- Seam P, Juweid ME, Cheson BD. The role of FDG-PET scans in patients with lymphoma. *Blood*. 2007;110:3507–3516.
- Kuenzle K, Taverna C, Steinert HC. Detection of extramedullary infiltrates in acute myelogenous leukemia with whole-body positron emission tomography and 2-deoxy-2- ^{18}F -fluoro-D-glucose. *Mol Imaging Biol*. 2002;4:179–183.
- Wells P, Gunn RN, Alison M, et al. Assessment of proliferation in vivo using 2- ^{11}C thymidine positron emission tomography in advanced intra-abdominal malignancies. *Cancer Res*. 2002;62:5698–5702.
- Martiat P, Ferrant A, Labar D, et al. In vivo measurement of carbon-11 thymidine uptake in non-Hodgkin's lymphoma using positron emission tomography. *J Nucl Med*. 1988;29:1633–1637.
- Shields AF, Grierson JR, Dohmen BM, et al. Imaging proliferation in vivo with ^{18}F FLT and positron emission tomography. *Nat Med*. 1998;4:1334–1336.
- Buck AK, Bommer M, Stilgenbauer S, et al. Molecular imaging of proliferation in malignant lymphoma. *Cancer Res*. 2006;66:11055–11061.
- Agool A, Schot BW, Jager PL, Vellenga E. ^{18}F -FLT PET in hematologic disorders: a novel technique to analyze the bone marrow compartment. *J Nucl Med*. 2006;47:1592–1598.
- Reske SN, Deisenhofer S, Glatting G, et al. ^{123}I -ITdU-mediated nanoirradiation of DNA efficiently induces cell kill in HL60 leukemia cells and in doxorubicin-, beta-, or gamma-radiation-resistant cell lines. *J Nucl Med*. 2007;48:1000–1007.
- Jaffe ES, Harris NL, Stein H. World Health Organization: classification of tumours—pathology and genetics of tumours of haematopoietic and lymphoid tissues. Lyon, France: IARC Press; 2001.
- Machulla HJ, Blocher A, Kuntzsch M. Simplified labeling approach for synthesizing 3'-deoxy-3'- ^{18}F fluorothymidine (^{18}F FLT). *J Radioanal Nucl Chem*. 2000;24:843–846.
- Buck AK, Schirrmeister H, Hetzel M, et al. 3-deoxy-3'- ^{18}F fluorothymidine-positron emission tomography for noninvasive assessment of proliferation in pulmonary nodules. *Cancer Res*. 2002;62:3331–3334.
- Schmidlin P. Improved iterative image reconstruction using variable projection binning and abbreviated convolution. *Eur J Nucl Med*. 1994;21:930–936.
- Rasey JS, Grierson JR, Wiens LW, Kolb PD, Schwartz JL. Validation of FLT uptake as a measure of thymidine kinase-1 activity in A549 carcinoma cells. *J Nucl Med*. 2002;43:1210–1217.
- Wagner M, Seitz U, Buck A, et al. 3'- ^{18}F fluoro-3'-deoxythymidine (^{18}F FLT) as positron emission tomography tracer for imaging proliferation in a murine B-cell lymphoma model and in the human disease. *Cancer Res*. 2003;63:2681–2687.
- Jacobs AH, Thomas A, Kracht LW, et al. ^{18}F -fluoro-L-thymidine and ^{11}C -methylmethionine as markers of increased transport and proliferation in brain tumors. *J Nucl Med*. 2005;46:1948–1958.
- Jahns-Streubel G, Reuter C, Auf der Landwehr U, et al. Activity of thymidine kinase and of polymerase alpha as well as activity and gene expression of deoxycytidine deaminase in leukemic blasts are correlated with clinical response in the setting of granulocyte-macrophage colony-stimulating factor-based priming before and during TAD-9 induction therapy in acute myeloid leukemia. *Blood*. 1997;90:1968–1976.
- O'Neill KL, Zhang F, Li H, Fuja DG, Murray BK. Thymidine kinase 1: a prognostic and diagnostic indicator in ALL and AML patients. *Leukemia*. 2007;21:560–563.
- Wiley JS, Snook MB, Jamieson GP. Nucleoside transport in acute leukaemia and lymphoma: close relation to proliferative rate. *Br J Haematol*. 1989;71:203–207.
- Buck AK, Kratochwil C, Glatting G, et al. Early assessment of therapy response in malignant lymphoma with the thymidine analogue ^{18}F FLT. *Eur J Nucl Med Mol Imaging*. 2007;34:1775–1782.
- Barthel H, Cleij MC, Collingridge DR, et al. 3'-deoxy-3'- ^{18}F fluorothymidine as a new marker for monitoring tumor response to antiproliferative therapy in vivo with positron emission tomography. *Cancer Res*. 2003;63:3791–3798.
- Leyton J, Latigo JR, Perumal M, Dhaliwal H, He Q, Aboagye EO. Early detection of tumor response to chemotherapy by 3'-deoxy-3'- ^{18}F fluorothymidine positron emission tomography: the effect of cisplatin on a fibrosarcoma tumor model in vivo. *Cancer Res*. 2005;65:4202–4210.
- Herrmann K, Wieder HA, Buck AK, et al. Early response assessment using 3'-deoxy-3'- ^{18}F fluorothymidine-positron emission tomography in high-grade non-Hodgkin's lymphoma. *Clin Cancer Res*. 2007;13:3552–3558.
- Chen W, Delaloye S, Silverman DH, et al. Predicting treatment response of malignant gliomas to bevacizumab and irinotecan by imaging proliferation with ^{18}F fluorothymidine positron emission tomography: a pilot study. *J Clin Oncol*. 2007;25:4714–4721.
- Pio BS, Park CK, Pietras R, et al. Usefulness of 3'- ^{18}F fluoro-3'-deoxythymidine with positron emission tomography in predicting breast cancer response to therapy. *Mol Imaging Biol*. 2006;8:36–42.
- Galmardini CM, Mackey JR, Dumontet C. Nucleoside analogues and nucleobases in cancer treatment. *Lancet Oncol*. 2002;3:415–424.
- Barthel H, Perumal M, Latigo J, et al. The uptake of 3'-deoxy-3'- ^{18}F fluorothymidine into L5178Y tumours in vivo is dependent on thymidine kinase 1 protein levels. *Eur J Nucl Med Mol Imaging*. 2005;32:257–263.
- Perumal M, Pillai RG, Barthel H, et al. Redistribution of nucleoside transporters to the cell membrane provides a novel approach for imaging thymidylate synthase inhibition by positron emission tomography. *Cancer Res*. 2006;66:8558–8564.